Weighted ENO Schemes for Hamilton-Jacobi Equations

Guang-Shan Jiang[1] and Danping Peng[2]

Department of Mathematics
University of California at Los Angeles
Los Angeles, CA 90095-1555

Abstract

In this paper, we present a weighted ENO (essentially non-oscillatory) scheme to approximate the viscosity solution of the Hamilton-Jacobi equation:

$$\phi_t + H(x_1, \cdots, x_d, t, \phi, \phi_{x_1}, \cdots, \phi_{x_d}) = 0.$$

This weighted ENO scheme is constructed upon and has the same stencil nodes as the 3^{rd} order ENO scheme but can be as high as 5^{th} order accurate in the smooth part of the solution. In addition to the accuracy improvement, numerical comparisons between the two schemes also demonstrate that, the weighted ENO scheme is more robust than the ENO scheme.

Key words. ENO, weighted ENO, Hamilton-Jacobi equation, shape from shading, level set.

AMS(MOS) subject classification. 35L99, 65M06.

1 Introduction

The Hamilton-Jacobi equation:

$$\phi_t + H(x, t, \phi, D\phi) = 0, \qquad \phi(x, 0) = \phi_0(x) \tag{1.1}$$

[1]Research supported by ONR N00014-92-J-1890. Email: gsj@math.ucla.edu.

[2]Research supported by NSF DMS-94 04942. Email: dpeng@math.ucla.edu.

where $x \in R^d, t > 0$, arises in many applications such as variational calculus, optimal control, differential games, geometric optics and image processing. It is well known that the solutions to (1.1) typically are continuous but with discontinuous derivatives even when the initial condition $\phi_0(x)$ is smooth, and such solutions are in general not unique. In the celebrated work of Crandall and Lions [3], the notion of viscosity solution, which generalizes the classical solution, was introduced. Under mild assumptions on the Hamiltonian H and the initial function ϕ_0, the authors proved the existence, uniqueness and stability of the viscosity solution for (1.1). Since then, Hamilton-Jacobi equations have been intensively studied. Interested readers can consult the review paper by Crandall et al. [2] for references to recent developments.

The study of numerical approximations to the viscosity solution of (1.1) was started also by Crandall and Lions. In [4], they introduced an important class of monotone schemes for a simplified form of equation (1.1):

$$\phi_t + H(D\phi) = 0, \qquad \phi(x,0) = \phi_0(x) \tag{1.2}$$

and proved that these schemes converge to the viscosity solution. Unfortunately monotone schemes can be at most first order accurate, thus are too dissipative for most practical applications. Nevertheless, they can serve as building blocks for high order schemes. In [10], Osher and Sethian constructed a class of high order upwinding type schemes for equation (1.2), mimicking high order ENO(essentially non-oscillatory) schemes developed by Harten et al. [5, 15] for approximating conservation laws. Their construction was based on the observation that Hamilton-Jacobi equations are closely related to conservation laws. To see this, let ϕ be a solution to the 1D Hamilton-Jacobi equation $\phi_t + H(\phi_x) = 0$, then $u = \phi_x$ becomes a solution to the 1D conservation law $u_t + H(u)_x = 0$. Although such a relation does not exist in multi-dimensions, numerical schemes can be constructed through a dimension by dimension extension of the one dimensional scheme. The above idea was pursued further by Osher and Shu [11], where a general framework for constructing high order ENO schemes for (1.2) was given, together with several "building blocks" or monotone fluxes such as the global Lax-Friedrichs flux, the Godunov flux and the Roe flux with entropy fix. We want to point out that all the schemes above can be generalized in a straight-forward manner to solve the general equation (1.1). A little caution, however, needs to be taken due to the presence of ϕ in the Hamiltonian H. See Souganidis [16] for details.

In this paper, we construct a high order accurate weighted ENO (WENO) scheme for approximating the general Hamilton-Jacobi equation (1.1), following a similar approach of [11]. WENO schemes were initiated by Liu et al. [8] and later improved by Jiang and

Shu [6], both for the approximation of hyperbolic conservation laws. Roughly speaking, WENO schemes are central schemes in regions where the solution is smooth but emulate ENO schemes near the singularities of the solution. This is achieved by *weighting* the substencils of the base ENO scheme with the weights adapted to the relative smoothness of the solution on these substencils. The weights vary smoothly with respect to some *smoothness measurements* of the solution on each substencils, thus eliminate or alleviate the problems(e.g. linear instability, accuracy degeneracy, see [13]) caused by abrupt stencil changes in ENO schemes. Extensive shock calculations have demonstrated that WENO schemes are more accurate and robust than the base ENO schemes and enjoy a compact stencil relative to the order of accuracy, which may be very desirable for certain boundary treatments.

The paper is organized as follows: In Section 2, we present the WENO schemes in two steps: first, in Section 2.1, we compare the core idea of WENO schemes with that of ENO schemes in the context of approximating the first derivative of a function in one space dimension. Then in Section 2.2, we present the complete WENO scheme for the Hamilton-Jacobi equation in two space dimensions. The generalization to high space dimensions is straight forward. In Section 3, we apply the WENO scheme on a set of model problems, drawn from several areas of applications such as image processing, optimal control and recent level set calculations. Some remarks are made in Section 4.

2 The WENO Schemes

2.1 The Core Idea

Let ϕ be a Lipschitz continuous function in R^1 with piecewise smooth derivatives. We assume that the discontinuities of the derivatives of ϕ, if any, are isolated. Let x_k be a discretization of R^1 with uniform spacing Δx. We introduce

$$\phi_k = \phi(x_k), \qquad \Delta^+\phi_k = \phi_{k+1} - \phi_k, \qquad \Delta^-\phi_k = \phi_k - \phi_{k-1}. \tag{2.1}$$

To approximate $\phi_x(x_i)$ on a left-biased stencil $\{x_k, k = i-3, \cdots, i+2\}$, the 3^{rd} order accurate ENO scheme will choose one from the following

$$\begin{aligned} \phi^{-,0}_{x,i} &= \frac{1}{3}\frac{\Delta^+\phi_{i-3}}{\Delta x} - \frac{7}{6}\frac{\Delta^+\phi_{i-2}}{\Delta x} + \frac{11}{6}\frac{\Delta^+\phi_{i-1}}{\Delta x} \\ \phi^{-,1}_{x,i} &= -\frac{1}{6}\frac{\Delta^+\phi_{i-2}}{\Delta x} + \frac{5}{6}\frac{\Delta^+\phi_{i-1}}{\Delta x} + \frac{1}{3}\frac{\Delta^+\phi_i}{\Delta x} \end{aligned} \tag{2.2}$$

$$\phi^{-,2}_{x,i} \quad = \quad \frac{1}{3}\frac{\Delta^+\phi_{i-1}}{\Delta x} + \frac{5}{6}\frac{\Delta^+\phi_i}{\Delta x} - \frac{1}{6}\frac{\Delta^+\phi_{i+1}}{\Delta x}$$

where $\phi^{-,s}_{x,i}$ is the 3^{rd} order approximation to $\phi_x(x_i)$ based on the s^{th} substencil $\{x_k, k = i+s-3, \cdots, i+s\}$ for $s = 0, 1, 2$. See Figure 1(a). Which $\phi^{-,s}_{x,i}$ to choose is determined

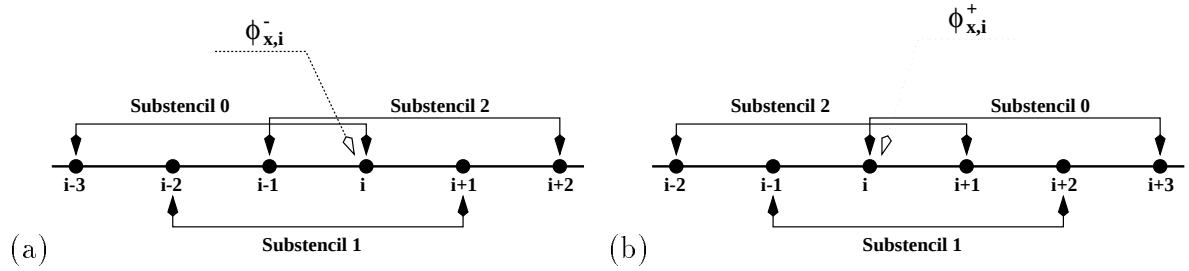

Figure 1: The three substencils. (a) The left-biased stencil; (b) The right-biased stencil.

by the relative "smoothness" of ϕ on the substencils. The 3^{rd} order ENO approximation to $\phi_x(x_i)$ is given as follows:

$$\phi^-_{x,i} = \begin{cases} \phi^{-,0}_{x,i} & \text{if } |\Delta^-\Delta^+\phi_{i-1}| < |\Delta^-\Delta^+\phi_i| \text{ and } |\Delta^-\Delta^-\Delta^+\phi_{i-1}| < |\Delta^+\Delta^-\Delta^+\phi_{i-1}|; \\ \phi^{-,2}_{x,i} & \text{if } |\Delta^-\Delta^+\phi_{i-1}| > |\Delta^-\Delta^+\phi_i| \text{ and } |\Delta^-\Delta^-\Delta^+\phi_i| > |\Delta^+\Delta^-\Delta^+\phi_i|; \\ \phi^{-,1}_{x,i} & \text{otherwise.} \end{cases} \tag{2.3}$$

The WENO approximation of $\phi_x(x_i)$ is instead a convex combination or weighted average of $\phi^{-,s}_{x,i} (s = 0, 1, 2)$:

$$\phi^-_{x,i} = \omega_0\phi^{-,0}_{x,i} + \omega_1\phi^{-,1}_{x,i} + \omega_2\phi^{-,2}_{x,i} \tag{2.4}$$

Here $\omega_s \geq 0$ is the weight associated with the s^{th} substencil and the weights satisfy the consistency equality: $\omega_0 + \omega_1 + \omega_2 = 1$. We will define these weights shortly.

If we set $\omega_0 = C_0 = 0.1, \omega_1 = C_1 = 0.6, \omega_2 = C_2 = 0.3$, we get

$$\frac{1}{30}\frac{\Delta^+\phi_{i-3}}{\Delta x} - \frac{13}{60}\frac{\Delta^+\phi_{i-2}}{\Delta x} + \frac{47}{60}\frac{\Delta^+\phi_{i-1}}{\Delta x} + \frac{9}{20}\frac{\Delta^+\phi_i}{\Delta x} - \frac{1}{20}\frac{\Delta^+\phi_{i+1}}{\Delta x} \tag{2.5}$$

which is the 5^{th} order approximation to $\phi_x(x_i)$ and is known to provide the smallest truncation error on such a six-point stencil. If we set the weight for the ENO chosen stencil to be unity and the remaining two weights to be zero, then (2.4) recovers the 3^{rd} order ENO approximation to $\phi_x(x_i)$. In case that there is a discontinuity inside the stencil, the ENO scheme can effectively choose relatively the "smoothest" stencil for the approximation thus avoid undue oscillations. To sustain both accuracy and essentially non-oscillatory property, we define the weights according to the following two principles: (1) if ϕ is smooth on the

whole stencil, then we require $\omega_s = C_s + O(\Delta x^2)$, in which case the WENO approximation (2.4) is uniformly 5^{th} order accurate. (2) if the stencil contains a singularity of ϕ, the weights adaptively approach the ENO "digital" (1 or 0) weights to avoid oscillations.

Substitute $\omega_1 = 1 - \omega_0 - \omega_2$ into (2.4), we get

$$\begin{aligned}\phi^-_{x,i} &= \omega_0\phi^{-,0}_{x,i} + (1-\omega_0-\omega_2)\phi^{-,1}_{x,i} + \omega_2\phi^{-,2}_{x,i} \\ &= \frac{1}{2}(\phi^{-,1}_{x,i} + \phi^{-,2}_{x,i}) + \omega_0(\phi^{-,0}_{x,i} - \phi^{-,1}_{x,i}) + (\omega_2 - \frac{1}{2})(\phi^{-,2}_{x,i} - \phi^{-,1}_{x,i})\end{aligned}$$

Notice that the first term does not depend on ω_s. Substitute $\phi^{-,s}_{x,i}$ in (2.2) into the last equation, we obtain

$$\begin{aligned}\phi^-_{x,i} &= \frac{1}{12}\left(-\frac{\Delta^+\phi_{i-2}}{\Delta x} + 7\frac{\Delta^+\phi_{i-1}}{\Delta x} + 7\frac{\Delta^+\phi_i}{\Delta x} - \frac{\Delta^+\phi_{i+1}}{\Delta x}\right) \\ &- \Phi^{WENO}\left(\frac{\Delta^-\Delta^+\phi_{i-2}}{\Delta x}, \frac{\Delta^-\Delta^+\phi_{i-1}}{\Delta x}, \frac{\Delta^-\Delta^+\phi_i}{\Delta x}, \frac{\Delta^-\Delta^+\phi_{i+1}}{\Delta x}\right) \qquad (2.6)\end{aligned}$$

where

$$\Phi^{WENO}(a,b,c,d) = \frac{1}{3}\omega_0(a-2b+c) + \frac{1}{6}(\omega_2 - \frac{1}{2})(b-2c+d) \qquad (2.7)$$

and the weights ω_0, ω_2 are defined as

$$\omega_0 = \frac{\alpha_0}{\alpha_0+\alpha_1+\alpha_2}, \qquad \omega_2 = \frac{\alpha_2}{\alpha_0+\alpha_1+\alpha_2}.$$

$$\alpha_0 = \frac{1}{(\epsilon + IS_0)^2}, \qquad \alpha_1 = \frac{6}{(\epsilon + IS_1)^2}, \qquad \alpha_2 = \frac{3}{(\epsilon + IS_2)^2}.$$

$$\begin{aligned}IS_0 &= 13(a-b)^2 + 3(a-3b)^2 \\ IS_1 &= 13(b-c)^2 + 3(b+c)^2 \\ IS_2 &= 13(c-d)^2 + 3(3c-d)^2\end{aligned}$$

Here ϵ is used to prevent the denominators from becoming zero. In our computation, we shall use $\epsilon = 10^{-6}$. One can check that the above definition of weights satisfies the two principles we mentioned in the previous paragraph. See [6] for details.

We can put the 3^{rd} ENO approximation (2.3) in a similar form as (2.6) with Φ^{WENO} replaced by

$$\Phi^{ENO}(a,b,c,d) = \begin{cases} \Phi_1 + \frac{1}{3}(a-2b+c) & \text{if } |b| < |c| \text{ and } |a-b| < |b-c|; \\ -\Phi_1 & \text{if } |b| > |c| \text{ and } |b-c| > |c-d|; \\ \Phi_1 & \text{otherwise.} \end{cases} \qquad (2.8)$$

where $\Phi_1 = -\frac{1}{12}(b - 2c + d)$.

By symmetry, the approximation of $\phi_x(x_i)$ on the right-biased stencil $\{x_k, k = i-2, \cdots, i+3\}$ (see Figure 1(b)), is

$$\begin{aligned} \phi^-_{x,i} &= \frac{1}{12}\left(-\frac{\Delta^+\phi_{i-2}}{\Delta x} + 7\frac{\Delta^+\phi_{i-1}}{\Delta x} + 7\frac{\Delta^+\phi_i}{\Delta x} - \frac{\Delta^+\phi_{i+1}}{\Delta x}\right) \\ &+ \Phi\left(\frac{\Delta^-\Delta^+\phi_{i+2}}{\Delta x}, \frac{\Delta^-\Delta^+\phi_{i+1}}{\Delta x}, \frac{\Delta^-\Delta^+\phi_i}{\Delta x}, \frac{\Delta^-\Delta^+\phi_{i-1}}{\Delta x}\right) \end{aligned} \tag{2.9}$$

where Φ is either Φ^{ENO} or Φ^{WENO}, corresponding to either ENO or WENO approximation.

To illustrate the differences between ENO and WENO schemes, we compute the weights in the approximation of $\phi_x(x_i)$ by $\phi^-_{x,i}$, where ϕ is given by

$$\phi(x) = \begin{cases} \frac{1}{2}(1 - \cos 2\pi x) & \text{if } 0 \le x \le \frac{1}{2}, \\ \pi(\frac{1}{2} - x) + \frac{1}{2}(3 + \cos 2\pi x) & \text{if } \frac{1}{2} < x \le 1. \end{cases}$$

and $x_i = i\Delta x, i = 0, 1, \cdots, 40, \Delta x = \frac{1}{40}$. Notice that all even derivatives of this function are discontinuous at $x = 0.5$. In addition, $\phi'' = 0$ at $x = 0.25, 0.75$. The results are shown in Figure 2. As we can see, the 3^{rd} order ENO switches stencil at the zeros of ϕ'' as well as the discontinuity of the derivatives of ϕ. On the other hand, the WENO scheme has the weights ω_s close to the optimal values(0.1 for ω_0, 0.6 for ω_1 and 0.3 for ω_2.), away from $x = 0.5$ (i.e. including at the points where $\phi'' = 0$); At $x = 0.5$, the weights are essentially equal to the ENO "digital" values.

Remark: Based on the 2^{nd} order ENO approximation, one can construct a 3^{rd} WENO approximation. This WENO approximation has a much simpler form than the 5^{th} order WENO one defined above. Here we provide the corresponding formulas for approximating $\phi_x(x_i)$. Interested readers can follow the approach described in the next subsection to obtain the 3^{rd} order WENO scheme. The approximation to $\phi_x(x_i)$ on the left-biased stencil $\{x_k, k = i-2, i-1, i, i+1\}$ is

$$\phi^-_{x,i} = \frac{1}{2}\left(\frac{\Delta^+\phi_{i-1}}{\Delta x} + \frac{\Delta^+\phi_i}{\Delta x}\right) - \frac{\omega_-}{2}\left(\frac{\Delta^+\phi_{i-2}}{\Delta x} - 2\frac{\Delta^+\phi_{i-1}}{\Delta x} + \frac{\Delta^+\phi_i}{\Delta x}\right).$$

where

$$\omega_- = \frac{1}{1 + 2r^2}, \qquad r = \frac{\epsilon + (\Delta^-\Delta^+\phi_{i-1})^2}{\epsilon + (\Delta^-\Delta^+\phi_i)^2}.$$

The approximation to $\phi_x(x_i)$ on the right-biased stencil $\{x_k, k = i-1, i, i+1, i+2\}$ is

$$\phi^+_{x,i} = \frac{1}{2}\left(\frac{\Delta^+\phi_{i-1}}{\Delta x} + \frac{\Delta^+\phi_i}{\Delta x}\right) + \frac{\omega_+}{2}\left(\frac{\Delta^+\phi_{i+1}}{\Delta x} - 2\frac{\Delta^+\phi_i}{\Delta x} + \frac{\Delta^+\phi_{i-1}}{\Delta x}\right).$$

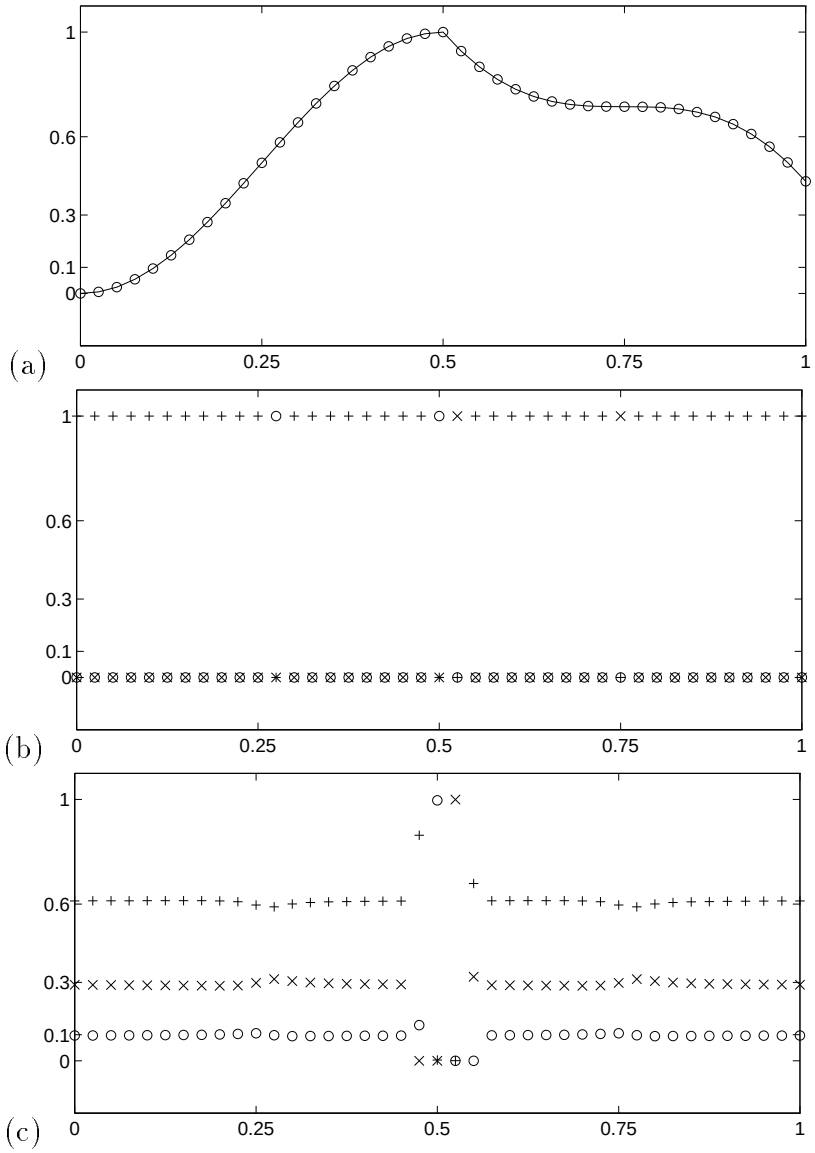

Figure 2: (a) The function ϕ; (b) The "weights" for ENO; (c) The weights for WENO. In (b,c), "o", "+" and "x" represent the weight for substencil $0, 1, 2$, respectively.

where

$$\omega_+ = \frac{1}{1+2r^2}, \qquad r = \frac{\epsilon + (\Delta^- \Delta^+ \phi_{i+1})^2}{\epsilon + (\Delta^- \Delta^+ \phi_i)^2}.$$

2.2 The WENO scheme in 2D

In this subsection, we use the 2D Hamilton-Jacobi equation

$$\phi_t + H(x, y, t, \phi, \phi_x, \phi_y) = 0 \tag{2.10}$$

as an example to describe the WENO scheme for multi-dimensional Hamilton-Jacobi equations. Let x_i, y_j be the (i, j) node of a 2D lattice grid with the uniform spacing Δx in x-direction and Δy in y-direction. Similar to the notations in (2.1), we introduce

$$\phi_{k,l} = \phi(x_k, y_l), \qquad \Delta_x^+ \phi_{k,l} = \phi_{k+1,l} - \phi_{k,l}, \qquad \Delta_y^+ \phi_{k,l} = \phi_{k,l+1} - \phi_{k,l}. \tag{2.11}$$

The semi-discrete form of the WENO scheme is

$$\frac{d\phi_{i,j}}{dt} = L(\phi)_{i,j} = -\hat{H}(x_i, y_j, t, \phi_{i,j}, \phi^+_{x,i,j}, \phi^-_{x,i,j}, \phi^+_{y,i,j}, \phi^-_{y,i,j}) \tag{2.12}$$

Here, $\phi^{\pm}_{x,i,j}$ are WENO approximations to $\frac{\partial \phi}{\partial x}(x_i, y_j)$ similar to the 1D approximations (2.6) and (2.9), i.e.

$$\begin{aligned} \phi^{\pm}_{x,i,j} &= \frac{1}{12}\left(-\frac{\Delta_x^+ \phi_{i-2,j}}{\Delta x} + 7\frac{\Delta_x^+ \phi_{i-1,j}}{\Delta x} + 7\frac{\Delta_x^+ \phi_{i,j}}{\Delta x} - \frac{\Delta_x^+ \phi_{i+1,j}}{\Delta x}\right) \\ &\pm \Phi^{WENO}\left(\frac{\Delta_x^- \Delta_x^+ \phi_{i\pm 2,j}}{\Delta x}, \frac{\Delta_x^- \Delta_x^+ \phi_{i\pm 1,j}}{\Delta x}, \frac{\Delta_x^- \Delta_x^+ \phi_{i,j}}{\Delta x}, \frac{\Delta_x^- \Delta_x^+ \phi_{i\mp 1,j}}{\Delta x}\right) \end{aligned} \tag{2.13}$$

$$\tag{2.14}$$

Similarly, $\phi^{\pm}_{y,i,j}$ are WENO approximations to $\frac{\partial \phi}{\partial y}(x_i, y_j)$ and are given by

$$\begin{aligned} \phi^{\pm}_{y,i,j} &= \frac{1}{12}\left(-\frac{\Delta_y^+ \phi_{i,j-2}}{\Delta y} + 7\frac{\Delta_y^+ \phi_{i,j-1}}{\Delta y} + 7\frac{\Delta_y^+ \phi_{i,j}}{\Delta y} - \frac{\Delta_y^+ \phi_{i,j+1}}{\Delta y}\right) \\ &\pm \Phi^{WENO}\left(\frac{\Delta_y^- \Delta_y^+ \phi_{i,j\pm 2}}{\Delta y}, \frac{\Delta_y^- \Delta_y^+ \phi_{i,j\pm 1}}{\Delta y}, \frac{\Delta_y^- \Delta_y^+ \phi_{i,j}}{\Delta y}, \frac{\Delta_y^- \Delta_y^+ \phi_{i,j\mp 1}}{\Delta y}\right) \end{aligned} \tag{2.15}$$

$$\tag{2.16}$$

Remark 1: If we replace Φ^{WENO} by Φ^{ENO} above, we obtain the 3^{rd} order ENO scheme.
Remark 2: $\hat{H}$ is a Lipschitz continuous monotone flux consistent with H:

$$\hat{H}(x, y, t, \phi, u, u, v, v) = H(x, y, t, \phi, u, v)$$

Monotonicity here means that $\hat{H}$ is nonincreasing in its fifth and seventh arguments and nondecreasing in its sixth and eighth arguments. There are many such fluxes. Here we take a couple of the most useful ones from Osher-Shu [11]. *In defining these fluxes, we omit the dependence of H on x, y, t, ϕ for simplicity.*

(1) The local Lax-Friedrichs(LLF) flux:

$$\hat{H}^{LLF}(u^+, u^-, v^+, v^-) = H(\frac{u^+ + u^-}{2}, \frac{v^+ + v^-}{2}) - \alpha(u^+, u^-)\frac{u^+ - u^-}{2} - \beta(v^+, v^-)\frac{v^+ - v^-}{2} \tag{2.17}$$

where

$$\alpha(u^+, u^-) = \max_{\substack{u \in I(u^-, u^+) \\ v \in [C,D]}} |H_1(u, v)|, \qquad \beta(v^+, v^-) = \max_{\substack{v \in I(v^-, v^+) \\ u \in [A,B]}} |H_2(u, v)|. \tag{2.18}$$

Here $H_1(H_2)$ stands for the partial derivative of H with respect to $\phi_x(\phi_y)$; $[A, B]$ is the value range for $u^{\pm}$ and $[C, D]$ is the value range for $v^{\pm}$; $I(a, b) = [\min(a, b), \max(a, b)]$. If we change $I(u^-, u^+)$ to $[A, B]$ and $I(v^-, v^+)$ to $[C, D]$ in (2.18), we obtain the global Lax-Friedrichs(LF) flux $\hat{H}^{LF}(u^+, u^-, v^+, v^-)$.

(2) Roe with entropy fix (RF) flux:

$$\hat{H}^{RF}(u^+, u^-, v^+, v^-) = \begin{cases} H(u^*, v^*) & \text{if } H_1(u, v) \text{ and } H_2(u, v) \text{ do not} \\ & \text{change sign in } u \in I(u^-, u^+) \\ & \text{and } v \in I(v^-, v^+); \\ H(\frac{u^+ + u^-}{2}, v^*) - \alpha(u^+, u^-)\frac{u^+ - u^-}{2} & \text{else if } H_2(u, v) \text{ does not change} \\ & \text{sign in } u \in [A, B],\ v \in I(v^-, v^+); \\ H(u^*, \frac{v^+ + v^-}{2}) - \beta(v^+, v^-)\frac{v^+ - v^-}{2} & \text{else if } H_2(u, v) \text{ does not change} \\ & \text{sign in } v \in [C, D],\ u \in I(u^-, u^+); \\ \hat{H}^{LLF}(u^+, u^-, v^+, v^-) & \text{otherwise.} \end{cases} \tag{2.19}$$

where u^*, v^* are defined by upwinding

$$u^* = \begin{cases} u^+ & \text{if } H_1(u, v) \le 0; \\ u^- & \text{if } H_1(u, v) \ge 0. \end{cases} \qquad v^* = \begin{cases} v^+ & \text{if } H_2(u, v) \le 0; \\ v^- & \text{if } H_2(u, v) \ge 0. \end{cases} \tag{2.20}$$

Remark 3: For time discretization, we use the Runge-Kutta schemes of Shu-Osher [14]. For the ODE

$$\frac{d\phi}{dt} = L(\phi)$$

the third order TVD(total variation non-increasing) Runge-Kutta is simply:

$$\begin{aligned}
\phi^{(1)} &= \phi^{(0)} + \Delta t L(\phi^{(0)}) \\
\phi^{(2)} &= \phi^{(1)} + \frac{\Delta t}{4}(-3L(\phi^{(0)}) + L(\phi^{(1)})) \\
\phi^{(3)} &= \phi^{(2)} + \frac{\Delta t}{12}(-L(\phi^{(0)}) - L(\phi^{(1)}) + 8L(\phi^{(2)}))
\end{aligned}$$

with $\phi^{(0)} = \phi^n$ and $\phi^{n+1} = \phi^{(3)}$. The fourth order non-TVD Runge-Kutta scheme is:

$$\begin{aligned}
\phi^{(1)} &= \phi^{(0)} + \frac{\Delta t}{2} L(\phi^{(0)}) \\
\phi^{(2)} &= \phi^{(1)} + \frac{\Delta t}{2}(-L(\phi^{(0)}) + L(\phi^{(1)})) \\
\phi^{(3)} &= \phi^{(2)} + \frac{\Delta t}{2}(-L(\phi^{(1)}) + 2L(\phi^{(2)})) \\
\phi^{(4)} &= \phi^{(3)} + \frac{\Delta t}{6}(L(\phi^{(0)}) + 2L(\phi^{(1)}) - 4L(\phi^{(2)}) + L(\phi^{(3)}))
\end{aligned}$$

with $\phi^{(0)} = \phi^n$ and $\phi^{n+1} = \phi^{(4)}$.

3 Numerical Results

In this section, we apply the 5^{th} order WENO scheme to a set of model problems. We also compare the results with those obtained by the base 3^{rd} order ENO scheme. We use WENO-x to refer to the 5^{th} order WENO scheme and similarly ENO-x to refer to the 3^{rd} order base ENO scheme, where "x" could be "LF" (global Lax-Friedrichs flux), "LLF" (local Lax-Friedrichs flux) and "RF" (Roe's flux with entropy fix). Unless stated otherwise, we shall use the 3^{rd} order Runge-Kutta scheme for the ENO schemes and the 4^{th} order Runge-Kutta scheme for the WENO schemes. For all compuations, the CFL number is taken as 0.6.

Example 1 (Accuracy test) We solve

$$\phi_t + H(\phi_x) = 0, \qquad \phi(x,0) = -cos\pi x, \qquad -1 \le x < 1. \tag{3.1}$$

with a convex H (Burgers' equation):

$$H(u) = \frac{(u+\alpha)^2}{2} \tag{3.2}$$

and a nonconvex flux H:

$$H(u) = -\cos(u + \alpha) \tag{3.3}$$

We take $\alpha = 1$ in our calculation. In both cases, the solution is smooth at $t = t_1 = 0.5/\pi^2$ and has discontinuous first order derivatives at $t = t_2 = 1.5/\pi^2$. In Table 1 and 2, we list the L_1 and L_∞ errors of the schemes WENO-RF and ENO-RF. At $t = t_2$, the errors are computed at a distance of 0.1 away from any discontinuities in the derivatives of the solution. We note that the exact solution can be obtained using characteristic methods for both cases. For both schemes, we use the 3^{th} order Runge-Kutta scheme in time. To realize 5^{th} order in time, we take $\Delta t \approx \Delta x^{5/3}$ in the case of WENO-RF. Such restrictive time step is only used for accuracy test purpose and will not be used in later examples. From Table 1 and 2, we can see that for both the convex and nonconvex flux, the ENO scheme achieves about 3^{rd} order accuracy while the WENO scheme achieves about 5^{th} order accuracy. WENO-LLF (ENO-LLF) obtains similar accuracy as WENO-RF (ENO-RF) for both cases. WENO-LF (ENO-LF) is slightly less accurate than WENO-RF (ENO-RF). Similar accuracy was observed for the two dimensional model problems in Example 2 of [11].

Example 2 (Linear equation) We solve the linear equation

$$\phi_t + \phi_x = 0, \qquad \phi(x, 0) = g(x - 0.5), \qquad -1 \le x < 1. \tag{3.4}$$

with periodic boundary condition. Here we choose

$$g(x) = -(\sqrt{3}/2+9/2+2\pi/3)(x+1)+\begin{cases} 2\cos(3\pi x^2/2) - \sqrt{3} & -1 < x < -\frac{1}{3}; \\ 3/2 + 3\cos 2\pi x & -\frac{1}{3} < x < 0; \\ 15/2 - 3\cos 2\pi x & 0 < x < \frac{1}{3}; \\ (28 + 4\pi + \cos 3\pi x)/3 + 6\pi \cos 3\pi x & \frac{1}{3} < x < 1. \end{cases} \tag{3.5}$$

This function is the integral of the function used by Harten et al. [5] modulo some linear function chosen so that $g(-1) = g(1)$. We shift the function to position the singular points of g inside the interval. The results at $t = 2, 8, 16, 32$ are displayed in Figure 3. We observe that, as the time increases, both the ENO scheme and the WENO scheme smooth out the corners in the graph of g. However, the WENO scheme performs much better at the smooth part of g. In fact even at the corners, the smoothing by the WENO scheme is less severe than that by the ENO scheme.

Table 1: L_1 and L_∞ errors for Example 1: Burgers' equation $H(u) = (u+1)^2/2$.

Scheme	N	L_∞ error	L_∞ order	L_1 error	L_1 order
$t = 0.5/\pi^2$					
ENO-RF	10	0.17E-01	-	0.60E-02	-
	20	0.39E-02	2.07	0.90E-03	2.73
	40	0.67E-03	2.55	0.13E-03	2.78
	80	0.86E-04	2.97	0.18E-04	2.87
	160	0.18E-04	2.25	0.26E-05	2.76
WENO-RF	10	0.59E-02	-	0.20E-02	-
	20	0.41E-03	3.86	0.84E-04	4.57
	40	0.39E-04	3.41	0.52E-05	4.02
	80	0.16E-05	4.58	0.22E-06	4.56
	160	0.61E-07	4.72	0.85E-08	4.69
$t = 1.5/\pi^2$					
ENO-RF	10	0.24E-01	-	0.84E-02	-
	20	0.61E-02	1.97	0.11E-02	2.93
	40	0.10E-02	2.60	0.13E-03	3.04
	80	0.11E-03	3.24	0.15E-04	3.14
	160	0.11E-04	3.30	0.19E-05	3.03
WENO-RF	10	0.83E-02	-	0.23E-02	-
	20	0.21E-02	1.98	0.20E-03	3.51
	40	0.17E-03	3.59	0.62E-05	5.02
	80	0.30E-05	5.86	0.11E-06	5.84
	160	0.80E-07	5.23	0.36E-08	4.94

Table 2: L_1 and L_∞ errors for Example 1: Nonconvex $H(u) = -\cos(u+1)$.

Scheme	N	L_∞ error	L_∞ order	L_1 error	L_1 order
$t = 0.5/\pi^2$					
ENO-RF	10	0.31E-02	-	0.11E-02	-
	20	0.12E-02	1.34	0.33E-03	1.77
	40	0.28E-03	2.16	0.61E-04	2.42
	80	0.49E-04	2.51	0.90E-05	2.76
	160	0.67E-05	2.86	0.12E-05	2.88
WENO-RF	10	0.28E-02	-	0.15E-02	-
	20	0.45E-03	2.65	0.12E-03	3.67
	40	0.52E-04	3.09	0.73E-05	4.04
	80	0.44E-05	3.58	0.33E-06	4.45
	160	0.22E-06	4.28	0.14E-07	4.58
$t = 1.5/\pi^2$					
ENO-RF	10	0.16E-01	-	0.64E-02	-
	20	0.28E-02	2.50	0.69E-03	3.21
	40	0.45E-03	2.63	0.11E-03	2.66
	80	0.70E-04	2.66	0.16E-04	2.80
	160	0.12E-04	2.55	0.22E-05	2.84
WENO-RF	10	0.68E-02	-	0.30E-02	-
	20	0.15E-02	2.22	0.35E-03	3.07
	40	0.32E-03	2.20	0.28E-04	3.66
	80	0.26E-04	3.60	0.15E-05	4.17
	160	0.85E-06	4.96	0.38E-07	5.35

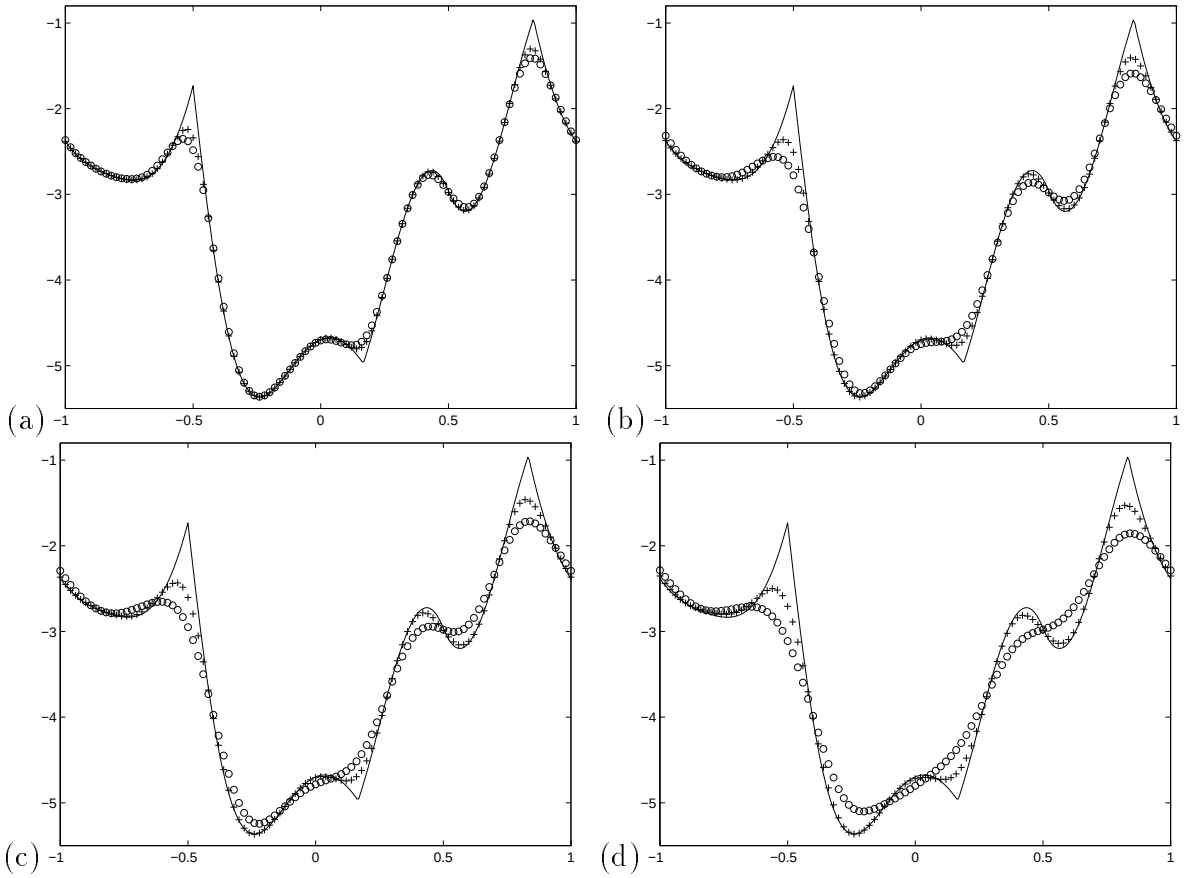

Figure 3: Linear equation. Solid line is the exact solution; "+" is by WENO-RF and "o" is by ENO-RF. (a) $t = 2$; (b) $t = 8$; (c) $t = 16$; (d) $t = 32$.

Example 3 (2D nonconvex Riemann problem) We solve a two-dimensional nonconvex Riemann problem(Example 3 of [11]):

$$\phi_t + \sin(\phi_x + \phi_y) = 0, \qquad \phi(x, y, 0) = \pi * (|y| - |x|) \tag{3.6}$$

using ENO-RF and WENO-RF. The results are displayed in Figure 4. We can see that both schemes capture the viscosity solution of the Riemann problem. For this problem, the advantage of the high accuracy of the WENO scheme is less obvious due to the almost piecewise linear structure of the solution.

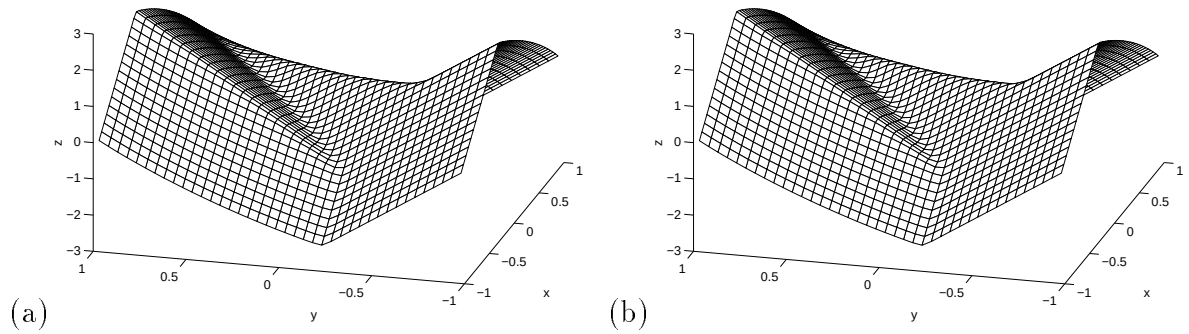

Figure 4: 2D nonconvex Riemann problem. 40×40. $t = 1$. (a) ENO-RF; (b) WENO-RF.

Example 4 (Optimal control) We solve the following problems related to control optimal cost determination [9, 11]:

$$\begin{aligned} &\phi_t - (\sin y)\phi_x + (\sin x + sign(\phi_y))\phi_y - \tfrac{1}{2}\sin^2 y - (1 - \cos x) = 0, \\ &\phi(x, y, 0) = 0. \end{aligned} \tag{3.7}$$

in $(x, y) \in [-\pi, \pi] \times [-\pi, \pi]$ with periodic boundary condition. The results at $t = 1$ are displayed in Figure 5. The difference between two schemes is hard to tell from the plots. The is partly because of the limitation of the graphical presentation and partly because of the short evolution time.

Example 5 (Shape from shading) We solve the following shape from shading problem:

$$\phi_t + I(x, y)\sqrt{1 + \phi_x^2 + \phi_y^2} - 1 = 0, \qquad (x, y) \in (0, 1) \times (0, 1). \tag{3.8}$$

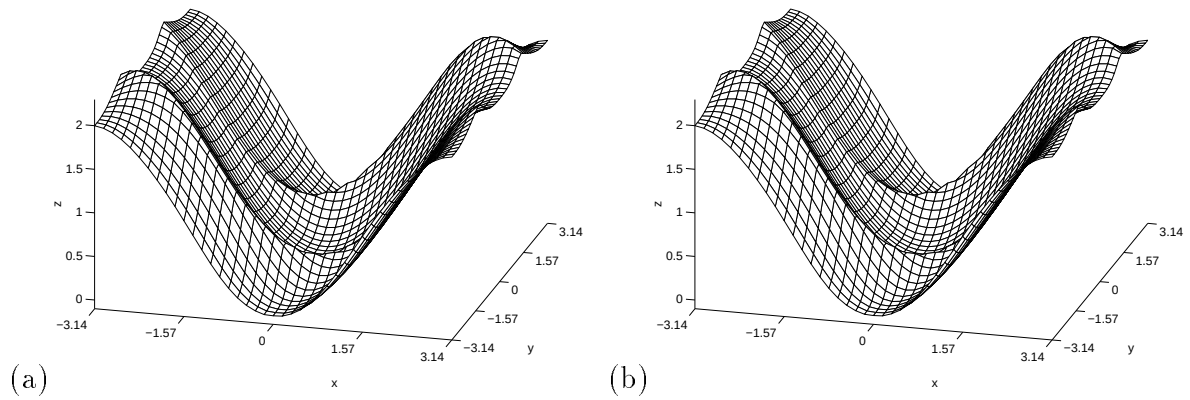

Figure 5: Optimal control. 40×40. $t = 1$. (a) ENO-RF; (b) WENO-RF.

Here $I(x, y)$ is the brightness value at (x, y), $0 < I(x, y) \leq 1$. In our problem, we take

$$I(x, y) = 1/\sqrt{1 + (2\pi \cos(2\pi x) \sin(2\pi y))^2 + (2\pi \sin(2\pi x) \cos(2\pi y))^2} \tag{3.9}$$

and $\phi(x, y, t) = 0$ at the boundary of the unit square. The steady state solution of (3.8) is the shape function, which has the brightness I under vertical lighting. See [12]. According to Lions et al. [7], there are multiple solutions to (3.8) and (3.9) and all satisfy the homogeneous boundary condition. In our problem, we need to prescribe additional "boundary conditions" at points where $I(x, y) = 1$.

We consider two such boundary conditions [12]:

(a) $\phi(\frac{1}{4}, \frac{1}{4}) = \phi(\frac{3}{4}, \frac{3}{4}) = 1, \phi(\frac{1}{4}, \frac{3}{4}) = \phi(\frac{3}{4}, \frac{1}{4}) = -1, \phi(\frac{1}{2}, \frac{1}{2}) = 0.$

(b) $\phi(\frac{1}{4}, \frac{1}{4}) = \phi(\frac{3}{4}, \frac{3}{4}) = \phi(\frac{1}{4}, \frac{3}{4}) = \phi(\frac{3}{4}, \frac{1}{4}) = 1, \phi(\frac{1}{2}, \frac{1}{2}) = 2.$

For case (a), the exact solution is $\phi(x, y) = \sin(2\pi x) \sin(2\pi y)$; We initialize the evolution by $\phi(x, y, 0) = (4096/9)xy(1-x)(1-y)(x-1/2)(y-1/2)$. The results are displayed in Figure 6.

For case (b), the exact solution is

$$\phi(x, y) = \begin{cases} \max\left(|\sin(2\pi x) \sin(2\pi y)|, 1 + \cos(2\pi x) \cos(2\pi y)\right) & \text{if } |x + y - 1| < \frac{1}{2} \\ & \text{and } |x - y| < \frac{1}{2}; \\ |\sin(2\pi x) \sin(2\pi y)| & \text{otherwise.} \end{cases}$$

We initialize the evolution by $\phi(x, y, 0) = 4 * \min(\min(x, 1 - x), \min(y, 1 - y))$. The results are displayed in Figure 7.

We observe that for case (a), where the solution is smooth, WENO-LF converges to steady state rapidly and the steady state solution is more accurate than that obtained by ENO-LF. ENO-LF can not converge to steady state even in this smooth case. For case (b), the exact solution is no longer smooth. WENO-LF is slightly more accurate than ENO-LF. However, neither scheme converges in this case. We believe this is due to the interesting extra boundary condition inside the domain. Special techniques may be needed to achieve convergence to the steady solution. We will investigate this issue elsewhere. Nevertheless, the numerical solution for both cases look smooth with no noticeable kinks, when compared to the results in [12].

Example 6 (Level set reinitialization) Consider

$$\begin{cases} \phi_t + sign(\phi_0)(\sqrt{\phi_x^2 + \phi_y^2} - 1) = 0 \quad \text{in } R^2 \times R_+ \\ \phi(x, y, 0) = \phi_0(x, y) \end{cases} \tag{3.10}$$

This equation first appeared in Sussman et al. [17], and since then, it has become very useful in reinitializing the level set function ϕ_0. Notice that the solution ϕ to (3.10) has the same zero level curve as that of ϕ_0 at all time, and it converges to the distance function to the zero level curve of ϕ_0 as t goes to infinity. In the level set formulation, ϕ_0 itself is governed by some evolution equation and its zero level curve is of critical importance. To accurately detect the zero level curve, it is necessary to keep ϕ_0 from being too flat or too steep. To compute the curvature of the level curves $\{\phi = constant\}$ from ϕ_0, which is often needed in physical applications, it is also important to keep ϕ_0 from being polluted by numerical noise. Ideally one would like to have ϕ_0 being the distance function to its zero level curve all the time. However, this is usually not guaranteed by the evolution equation for ϕ_0. Thus one periodically solves equation (3.10) and reset ϕ_0 to the steady state solution.

In our computation, we choose ϕ_0 to be the distance function to the circle centered at the origin with radius $\frac{1}{2}$, plus some small perturbation in both radial and angular directions near the circle:

$$\phi_0(x, y) = \begin{cases} d + \frac{\epsilon}{16\pi} \sin(\frac{4\pi d \sin 5\theta}{\epsilon}) & \text{if } |d| \le \epsilon; \\ d & \text{otherwise.} \end{cases} \tag{3.11}$$

where $d = \sqrt{x^2 + y^2} - 0.5, \theta = \tan^{-1}(y/x)$ and $\epsilon = 0.2$. We use the following Godunov flux:

$$H^G(u^+, u^-, v^+, v^-) = \begin{cases} s\sqrt{[\max((u^+)^-, (u^-)^+)]^2 + [\max((v^+)^-, (v^-)^+)]^2} & \text{if } \phi_{ij}^0 \ge 0; \\ s\sqrt{[\max((u^+)^+, (u^-)^-)]^2 + [\max((v^+)^+, (v^-)^-)]^2} & \text{otherwise.} \end{cases} \tag{3.12}$$

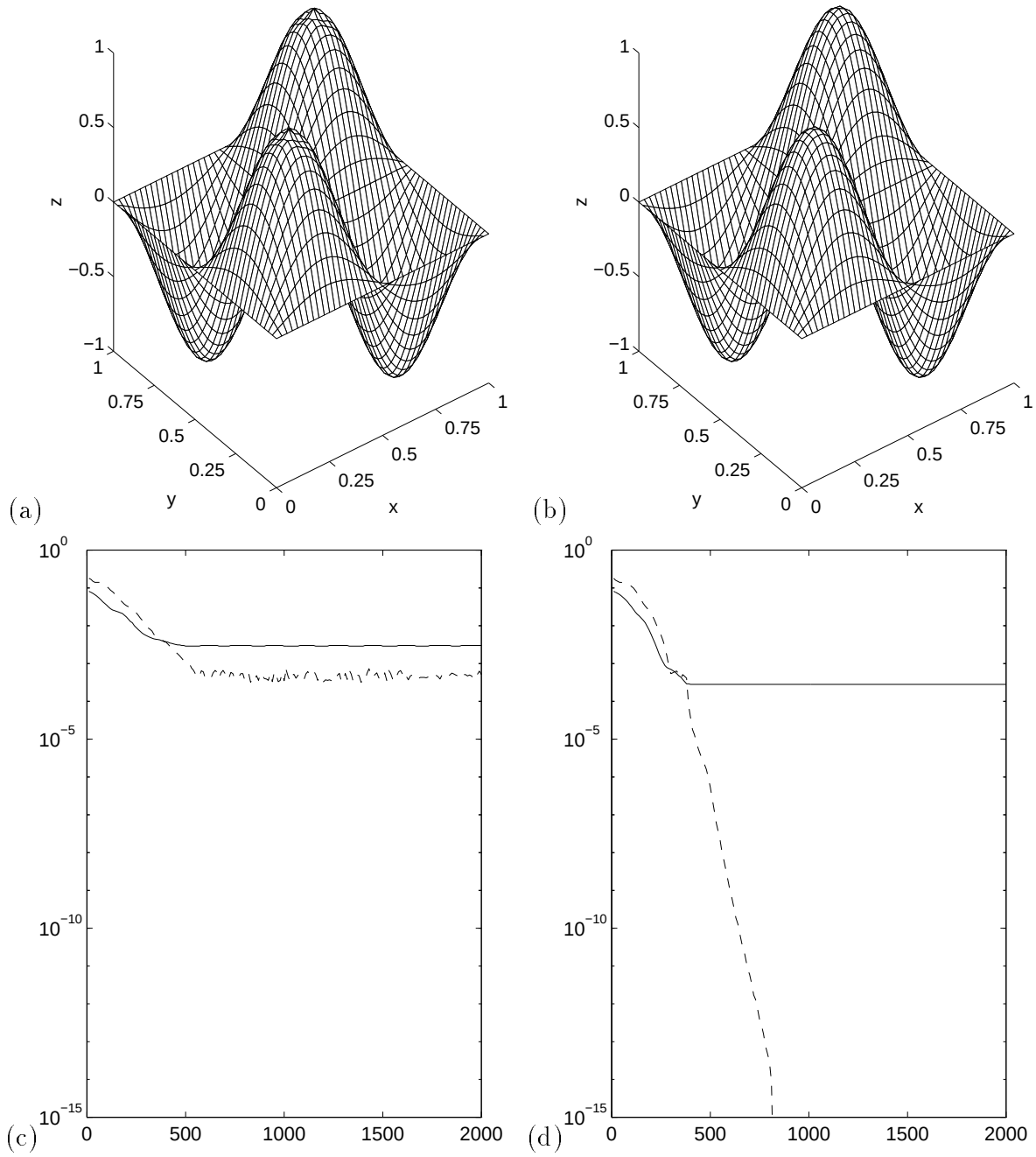

Figure 6: Shape from shading. Case (a). 40×40. (a) Shape function by ENO-LF; (b) Same as (a) but for WENO-LF; (c) ENO-LF, solid line: L_1 error, dashed line: L_1 norm of the residue; (d) Same as (d) but for WENO-LF.

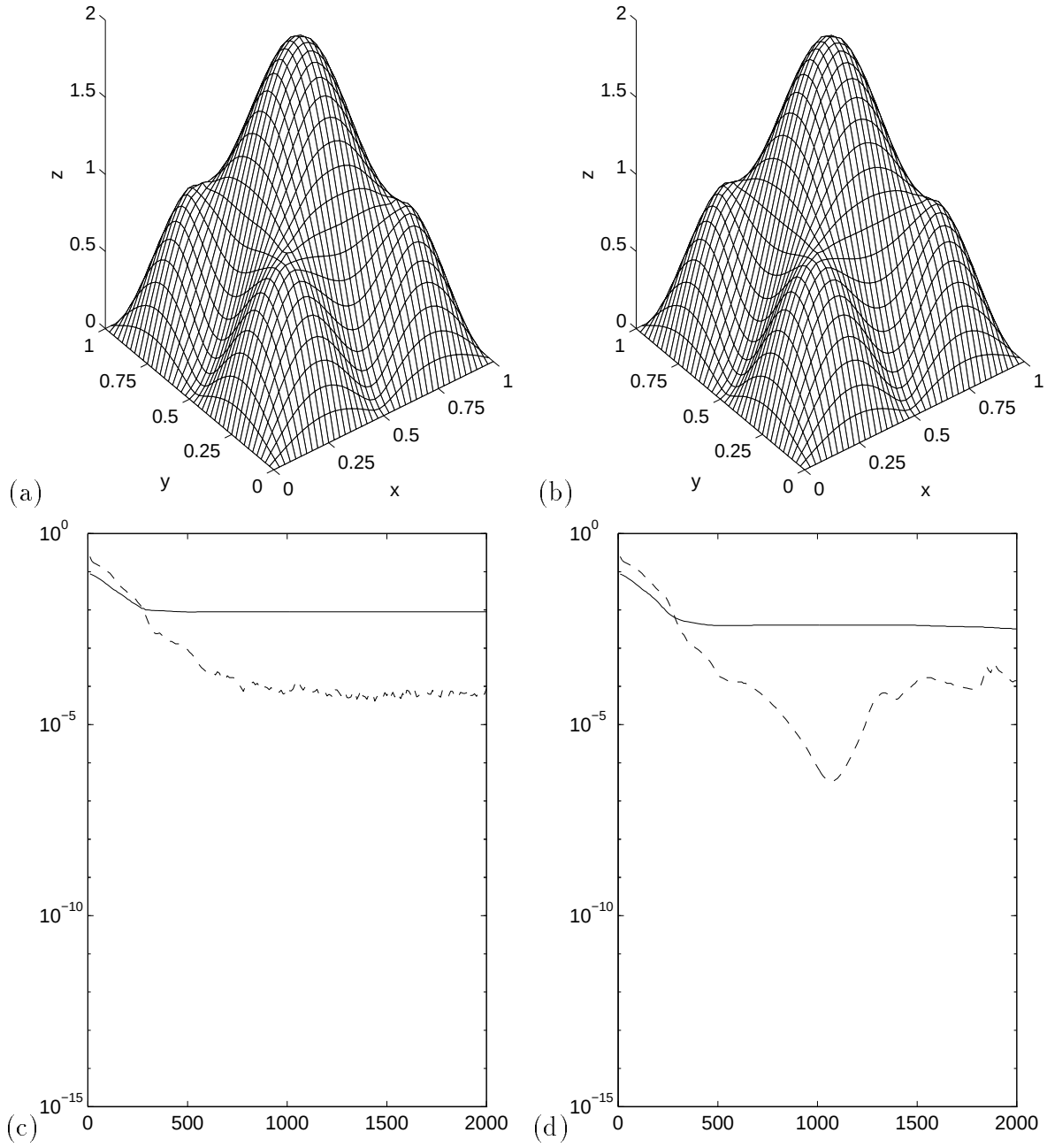

Figure 7: Shape from shading. Case (b). 40×40. (a) Shape function by ENO-LF; (b) Same as (a) but for WENO-LF; (c) ENO-LF, solid line: L_1 error, dashed line: L_1 norm of the residue; (d) Same as (d) but for WENO-LF.

where $\phi_{ij}^0 = \phi_0(x_i, y_j)$, $(a)^+ = max(a, 0)$ and $(a)^- = -min(a, 0)$. We also used $s = \phi_0/\sqrt{\phi_0^2 + \delta}$ to approximate $sign(\phi_0)$ with δ comparable to the spatial step size. It is worth pointing out that the Godunov flux is usually complicated for general Hamilton-Jacobi equations(see [1, 11]), but it has the above simple form for equation (3.10).

For both the ENO and WENO scheme, we use the 3^{rd} order Runge-Kutta scheme in time. We plot the level set function ϕ in Figure 8. To demonstrate the difference between the ENO and WENO scheme, we compute the curvature $\kappa \equiv \nabla \frac{\nabla \phi}{|\nabla \phi|}$ of the level curve $\{\phi = costant\}$ by central difference. The results are shown in Figure 9. From the numerical results, we observe the following:

- There is no distinguishable difference in ϕ before and after the reinitialization using either ENO or WENO scheme. However,
- There is significant difference between the curvature before and after the reinitialization. The latter is considerably smoother than the former for both ENO and WENO schemes.
- The curvature computed from the reinitialized data of ϕ by the WENO scheme is less noisy than that by the ENO scheme. Moreover, the WENO scheme does not deteriorate the level curves, which happens to the ENO scheme, as we continue the iteration further. We believe this is due to fact that WENO scheme smoothly weights the candidate stencils in contrast to the ENO scheme which jumps from one stencil to another abruptly even in the smooth part of the solution.

Although the WENO scheme does not remove the noise completely in the curvature, it is superior in this case than the ENO scheme. For problems sensitive to the curvature, the WENO scheme seems to be a better one to use.

4 Conclusion

We have presented a WENO scheme which is constructed upon the 3^{rd} order ENO scheme. This WENO scheme is uniformly 5^{th} order accurate in smooth regions but has the same stencil as the 3^{rd} order ENO scheme. Near singularities of the solution, the two schemes function similarly. The numerical experiments demonstrate that the gain of this accuracy does help long time integration. Moreover, the smooth weighting of the substencils in the WENO scheme helps prohibiting noises to be created in the solution. We believe that this

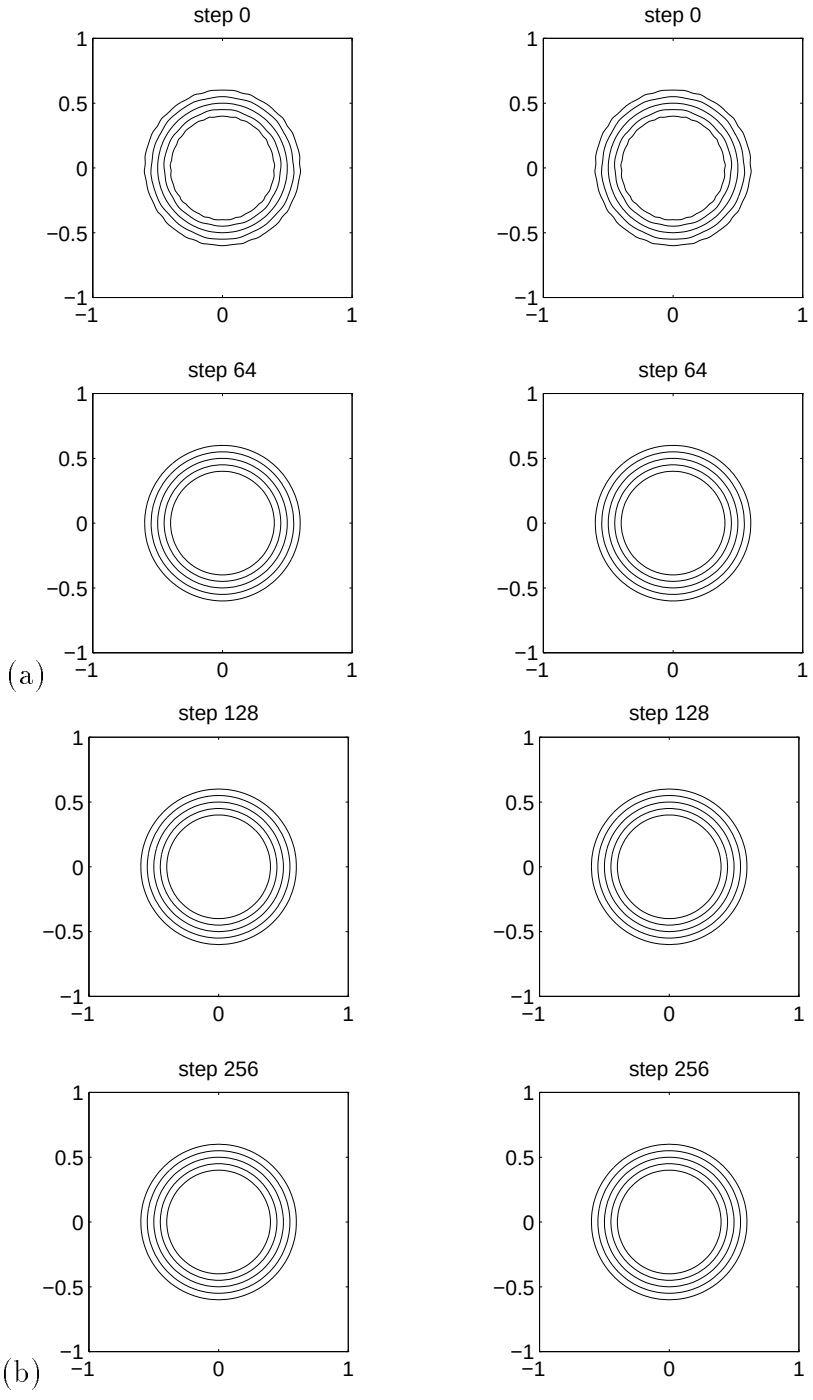

Figure 8: Level set reinitialization. 100×100. The contour of ϕ. Left column: ENO; Right column: WENO.

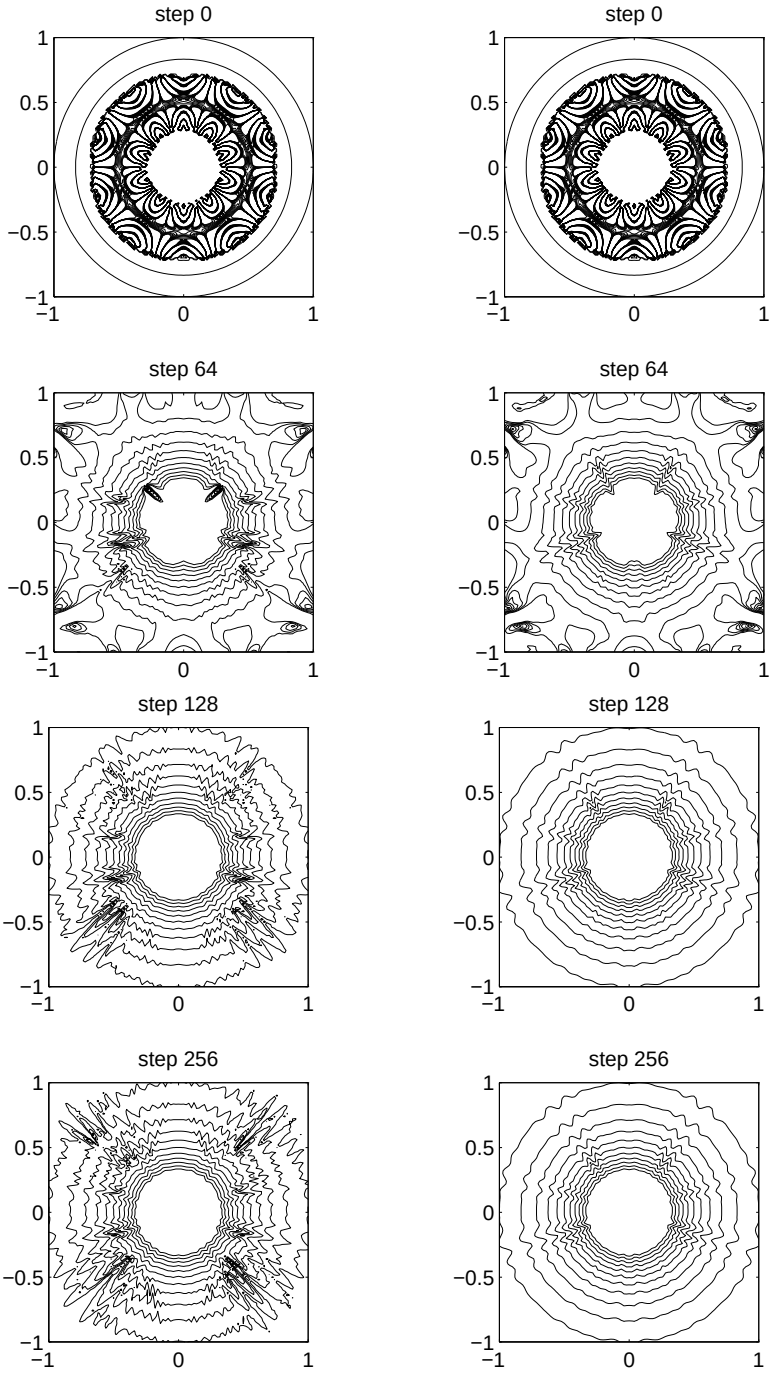

Figure 9: Level set reinitialization. 100×100. The contour plot of the curvature κ. Left column: ENO; Right column: WENO.

smooth weighting accounts most for the better performance of the WENO scheme over its base ENO scheme.

Based on the 2^{nd} order ENO scheme, one can also construct a 3^{rd} order WENO scheme. See the remark after Section 2.1.

5 Acknowledgments

We would like to thank Stanley Osher and Chi-Wang Shu for suggesting several test problems.

References

[1] M. Bardi and S. Osher, *The nonconvex multi-dimensional Riemann problem for Hamilton-Jacobi equations*, J. Numer. Anal., v22, 1991, pp. 344-351.

[2] M.G. Crandall, H. Ishii and P.L. Lions, *User's guide to viscosity solutions of second order partial equations*, Bulletin(New Series) of Amer. Math. Soc., v27, 1992, pp. 1-67.

[3] M.G. Crandall and P.L. Lions, *Viscosity solutions of Hamilton-Jacobi equations*, Trans. Americ. Math. Soc., v277, 1983, pp. 1-42.

[4] M.G. Crandall and P.L. Lions, *Two approximations of solutions of Hamilton-Jacobi equations*, Math. Comput., v43, 1984, pp. 1-19.

[5] A. Harten, B. Engquist, S. Osher and S. Chakravarthy, *Uniformly high-order accurate essentially non-oscillatory schemes III*, J. Comput. Phys., v71, 1987, pp. 231-303.

[6] G-S. Jiang and C.-W. Shu, *Efficient implementation of weighted ENO schemes* J. Comput. Phys., v126, 1996, pp. 202-228.

[7] P.L. Lions, E. Rouy and A. Tourin, *Shape-from-shading, viscosity solutions and edges*, Numer. Math., v64, 1993, pp. 323-353.

[8] X-D. Liu, S. Osher and T. Chan, *Weighted essentially non-oscillatory schemes*, J. Comput. Phys., v115, 1994, pp. 200-212.

[9] S. Osher, *A level set formulation for the solution of the Dirichlet problem for Hamilton-Jacobi equations*, J. Math. Anal., v24, 1993, pp. 1145-1152.

[10] S. Osher and J. Sethian, *Fronts propagating with curvature dependent speed: algorithms based on Hamilton-Jacobi formulations*, J. Comput. Phys., v79, 1988, pp. 12-49.

[11] S. Osher and C-W. Shu, *High-order essentially non-oscillatory schemes for Hamilton-Jacobi equations*, J. Numer. Anal., v28, 1991, pp. 907-922.

[12] E. Rouy and A. Tourin, *A viscosity solutions approach to shape-from-shading*, J. Numer. Anal., v29, 1992, pp. 867-884.

[13] C-W. Shu, *Numerical experiments on the accuracy of ENO and modified ENO schemes*, J. Sci. Comput., v5, 1990, pp. 127-150.

[14] C-W. Shu, *Total-variation-diminishing time discretizations*, SIAM J. Sci. Stat. Comput. v9, 1988, pp. 1073-1084.

[15] C-W. Shu and S. Osher, *Efficient implementation of essentially non-oscillatory shock-capturing schemes II*, J. Comput. Phys., v83, 1989, pp. 32-78.

[16] P.E. Souganidis, *Approximation schemes for viscosity solutions of Hamilton-Jacobi equations*, J. of Diff. Equations, v59, 1985, pp. 1-43.

[17] M. Sussman, P. Smereka and S. Osher, *A level set method for computing solutions to incompressible two-phase flow*, J. Comput. Phys., v114, 1994, pp. 146-159.